Efficient TCAD Temperature-dependent Large-Signal Simulation of a FinFET Power Amplifier

Efficient TCAD Temperature-dependent Large-Signal Simulation of a FinFET Power Amplifier

E. Catoggio[#1], S. Donati Guerrieri[#2], F. Bonani[#3], G. Ghione[#4],
[#]Dipartimento di Elettronica e Telecomunicazioni, Politecnico di Torino, Italy
{[1]eva.catoggio, [2]simona.donati, [3]fabrizio.bonani, [4]giovanni.ghione}@polito.it

***Abstract* — We show a complete temperature-dependent analysis of a low power FinFET-based class A amplifier for small-cell applications based on an efficient approach to the temperature-dependent physics-based analysis of electron devices in Large Signal (LS) nonlinear conditions. The method extends the Green's Function (GF) approach, already developed for the device LS noise and technological sensitivity, to calculate the LS device response to the temperature variation from a nominal, "cold" condition with a negligible numerical overhead with respect to the other GF-based analyses. T-dependent TCAD simulations are applied to assess the robustness of the FinFET-based power amplifier against device heating and load variations. Temperature variations dominate over load sensitivity, showing more than 1 dB output power loss and a PAE reduction from 28% to 23%. The proposed approach represents a first step towards the development of physically sound, temperature dependent, LS circuit models of nonlinear stages.**

***Keywords* — Semiconductor devices, Nonlinear device models, TCAD simulations, Harmonic Balance**

I. Introduction

Physics-based device simulations represent an ideal environment to accurately model the behavior of the active device in RF/microwave circuits, as they keep trace of the underlying technological and physical parameters. With the ever increasing capability of computation machines, the frequency domain analysis of electron devices operated in highly nonlinear conditions has proved to be a fairly manageable task even within TCAD simulators, especially using the Harmonic Balance formalism for mixed-mode simulations, where the device physical equations need to be solved concurrently with the external harmonic tuning circuits [1]–[3]. The outcome of Large Signal (LS) TCAD simulations can be also successfully integrated into circuit-level simulators through X-parameters [4], and further coupled to accurate Electro Magnetic (EM) simulations of the passive structures [5], thus making the physically based analysis of a complete nonlinear stage, such as a power amplifier, an attractive circuit simulation scenario. Nonetheless, to be successfully used for circuit analysis, the physics-based models must be able to predict the *sensitivity* of the nonlinear stage performance towards the variations of: 1) multiple physical/technological parameters (e.g. doping, geometry or material parameter spread); 2) variations of the embedding circuit (effectively corresponding to a load-pull analysis around the nominal load conditions); 3) temperature variations. Previously, we developed efficient numerical algorithms, based on the efficient computation of the Green's Functions of the device linearized physical model, to model the first two sources of variation [6]–[8]. In this work we address the problem of temperature variations, especially relevant in the scenario of power devices (e.g. GaAs or GaN based HEMTs) and nanoscale devices (e.g. FinFETs) [9], [10]. While self-consistent physics-based electro-thermal (ET) simulations, would be the ideal choice at the TCAD level [11], they meet fundamental limitations due to the numerical burden, especially in the nonlinear case. Full ET simulations can be simplified defining a device ("junction") temperature parametrizing the electrical model and self-heating is then accounted for through a self-consistent solution of the T-dependent electrical model coupled to an external thermal circuit. Hence, in this work we address the problem of T-dependent nonlinear simulations, where in the physical model a unique equivalent lattice temperature describes the overall device heating [12].

Our in-house code, allowing for the Harmonic Balance Large Signal analysis of electron devices, has been exended to account for the temperature dependency of the material properties, finally allowing for T-dependent LS simulations. The Conversion Matrix Green Function capability, originally developed for fast and numerically efficient LS noise, LS variability and synthetic load pull analyses, has been extendend accordingly [12]. The GF approach allows now for the fast and numerically efficient T-dependent LS analysis, starting from a single "cold" simulation. The variations with temperature can be easily coupled with other concurrent technological or load variations, finally allowing for an global assessment a nonlinear stage reliability.

In this paper, the novel code is used to simulate a FinFET-based power amplifier (PA) as a function of both temperature and load variations (akin to synthetic load-pull), showing that the GF approach is capable to accurately reproduce the LS stage performance up to 50 K temperature increase. We demonstrate that the stage is dominated by thermal degradation, showing more than 1 dB output power loss and PAE reduction from 28% to 23%.

II. Efficient T-dependent TCAD LS analysis

Consider an active device with N-ports connected to an N-port external load, as in Fig. 1 (left). The device constitutive equations collectively represent a physics-based model, e.g. the drift-diffusion equations, discretized over the device volume, and coupled to the external circuit, here represented by the equivalent load and power sources [13]. The system is

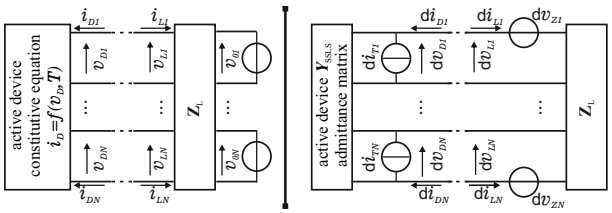

Fig. 1. Schematic representation of the linearized device including temperature induced and load-induced variations

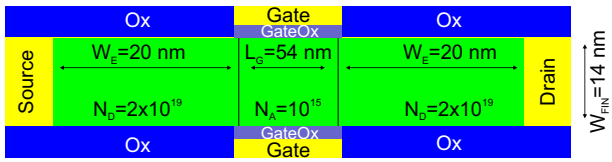

Fig. 2. Double Gate structure representing the cross-section of each elementary fin of the power cell.

linearized around the LS steady-state (nominal load $\mathbf{Z}_\mathrm{L}$ and "cold" temperature T_0), to account for a temperature variation δT in the physical model and a load variation $\delta\mathbf{Z}_\mathrm{L}$, yielding:

$$\delta\vec{i}_\mathrm{D} = \left.\frac{\partial f(\vec{v}_\mathrm{D},T)}{\partial \vec{v}_\mathrm{D}}\right|_0 \delta\vec{v}_\mathrm{D} + \left.\frac{\partial f(\vec{v}_\mathrm{D},T)}{\partial T}\right|_0 \delta T$$
$$= \mathbf{Y}_\mathrm{SSLS}\,\delta\vec{v}_\mathrm{D} + \delta\vec{i}_\mathrm{T}; \qquad (1)$$

$$\delta\vec{v}_\mathrm{L} = \mathbf{Z}_\mathrm{L}\,\delta\vec{i}_\mathrm{L} + \delta\mathbf{Z}_\mathrm{L}\;\vec{i}_\mathrm{L}\Big|_0 = \mathbf{Z}_\mathrm{L}\,\delta\vec{i}_\mathrm{L} + \delta\vec{v}_\mathrm{Z} \qquad (2)$$

where subscript "0" refers to the LS working point, "D" to the device ports, and "L" to the load ports . In (1)-(2), $\mathbf{Y}_\mathrm{SSLS}$ is the Small-Signal Large-Signal (SSLS) device admittance matrix, computed from SSLS TCAD analysis. The impressed generators $\delta\vec{i}_\mathrm{T}$ and $\delta\vec{v}_\mathrm{Z}$ collectively represent the equivalent terminal effect of δT and $\delta\mathbf{Z}_\mathrm{L}$. The linearized model allows for the representation in Fig. 1 (right).

With $\delta\vec{v}_\mathrm{L} = \delta\vec{v}_\mathrm{D}$ and $\delta\vec{i}_\mathrm{L} = -\delta\vec{i}_\mathrm{D}$, (1)-(2) yield

$$\delta\vec{i}_\mathrm{D} = (\mathbf{I} + \mathbf{Y}_\mathrm{SSLS}\mathbf{Z}_\mathrm{L})^{-1}\left(\delta\vec{i}_\mathrm{T} + \mathbf{Y}_\mathrm{SSLS}\delta\vec{v}_\mathrm{Z}\right) \qquad (3)$$

Generators $\delta\vec{v}_\mathrm{Z}$ are directly computed from the nominal LS solution using (2). Impressed generators $\delta\vec{i}_\mathrm{T}$, instead, are computed using the in-house TCAD simulator by means of the Conversion Matrix Green's Functions (CGF), with negligible numerical overhead with respect to the computation of the nominal LS working point: the details can be found in [6], [12]. For this work, the in-house code was extended to account for all temperature dependencies of the physical model, including mobility, velocity saturation and carrier statistics.

III. FinFET Power Amplifier

FinFET technology, primarly developed for digital applications, is being actively investigated for its possible applications in analog stages, being the natural evolution of the RF CMOS technology [14], [15]. For the exploitation of these extremely miniaturized devices in analog circuits, the impact of parasitics and the difficult thermal management are the primary concerns, calling for accurate nonlinear, self-heating oriented models. In the RF 5G scenario, small and medium power amplifiers are among the most challenging stages: here we propose the thermal analysis of a small power class A power amplifier operating at the frequency of 70 GHz. A unit cell made of a multifinger device (10 fingers of 30 fins each) with a fin height of 25 nm, corresponding to a total gate periphery of 15 μm, is used for the development of the power stage. More cells can be then combined to increase the output power.

The cross-section of each elementary fin of the power cell is represented in Fig. 2. This elementary structure was analyzed with our in-house 2D TCAD simulator to assess the power cell degradation with increasing temperature.

A preliminary device analysis was performed to select the DC bias $V_\mathrm{G} = 0.675$ V and $V_\mathrm{D} = 0.6$ V and the optimum load $Z_\mathrm{opt} = 53 + \mathrm{j}6\Omega$ according to the load-line approach. Notice that Z_opt has been calculated at the nominal "cold" temperature $T_0 = 300$ K, while at higher temperatures the device will exhibit a de-tuning due to the change of the ouput characteristics with T. The device was then simulated in large-signal conditions, with $n_\mathrm{H} = 10$ harmonics and increasing input power from back-off to 2 dB gain compression. Higher harmonics are supposed to be shorted at this high operating frequency. In this preliminary simulation campaign, the input port has been left unmatched and terminated with a 50 Ω/mm impedance.

A. T-dependent LS Analysis

We first address the stage temperature dependency with the nominal load condition, i.e. setting $\delta\mathbf{Z}_\mathrm{L} = 0$ in (2). At each input power, the CGFs are calculated at $T_0 = 300$ K and the drain current variation with T is evaluated according to (3) for 5 temperatures, spanning the interval $[310-350]$ K. GF results are verified against the reference solution, corresponding to repeated LS analyses with varying temperature (incremental method, INC). With the 5 temperatures under test, the simulation time of the INC analysis is roughly 5 times the one required for the GF approach (in this example, around 25 hours INC vs. 5 hours GF). All results show an excellent accuracy of the GF approach in all operating conditions.

Figs. 3 and 4 show the output power and gain of the power cell with increasing T. The power performance exhibits a noticeable degradation, with up to 1 dB less output power and gain at $T = 350$ K. The thermal sensitivity is higher in back-off and limited in compression: in fact, the variation of the output power above the 1 dB compression point is due to the knee voltage walk-out with T, which is in any case quite limited, see also Fig. 5 (solid line). Fig. 6 shows the stage efficiency (left) and its variation with respect to the "cold" case (right) as a function of the input power. The thermal sensitivity depends again on the input power having a maximum value at 1 dB compression, but a significant efficiency reduction is found in a wide range of output power (roughly from 5 dB OBO to saturation). This needs to be taken carefully into account in the design of quasi-linear stages, often operated with modulated signals whose average value is well in back-off.

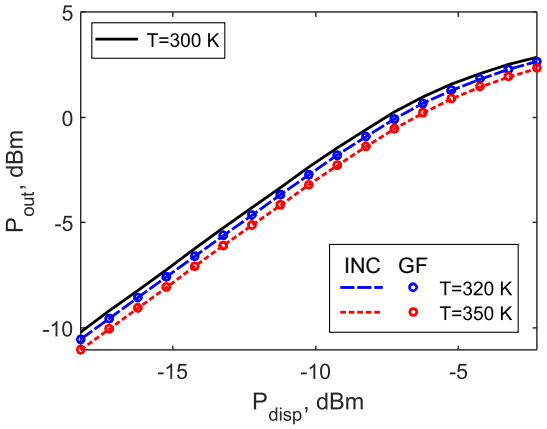

Fig. 3. $P_{\text{in}} - P_{\text{out}}$ plot for the class A PA as a function of temperature. Lines: incremental simulations at $T = 300$ K (solid), $T = 320$ K (dashed) and $T = 350$ K (dotted). Symbols: GF approach.

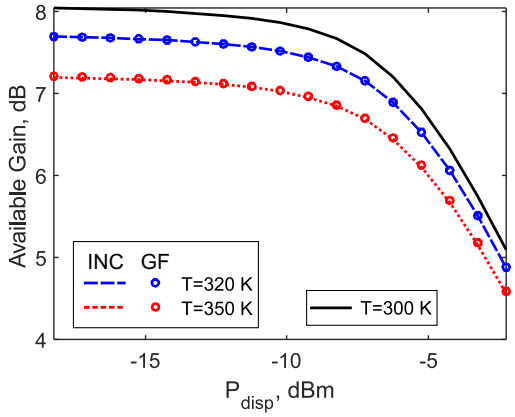

Fig. 4. Available Gain for the class A PA at varying temperature. Lines: incremental simulations at $T = 300$ K (solid), $T = 320$ K (dashed) and $T = 350$ K (dotted). Symbols: GF approach.

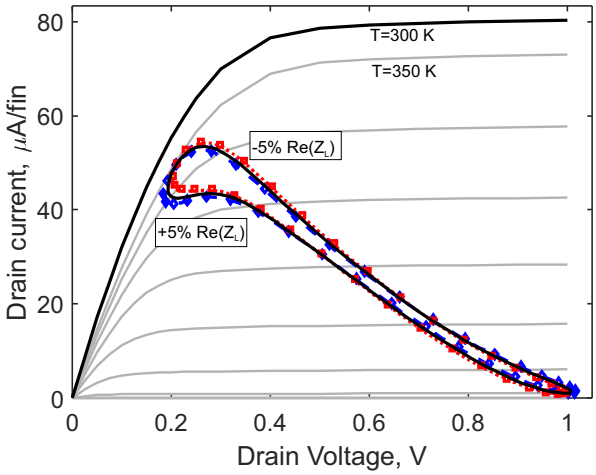

Fig. 5. Dynamic load lines at 2 dB gain compression, $T = 350$ K and varying the load condition. Black solid line: nominal load. Dotted line and squares: -5% variation of the nominal load real part. Dashed line and diamonds: $+5\%$ variation of the nominal load real part. Lines: incremental simulations. Symbols: GF approach. Output characteristics at $T = 350$ K are in grey, while the black output characteristic shows the "cold" case $T = 300$ K at the largest gate voltage.

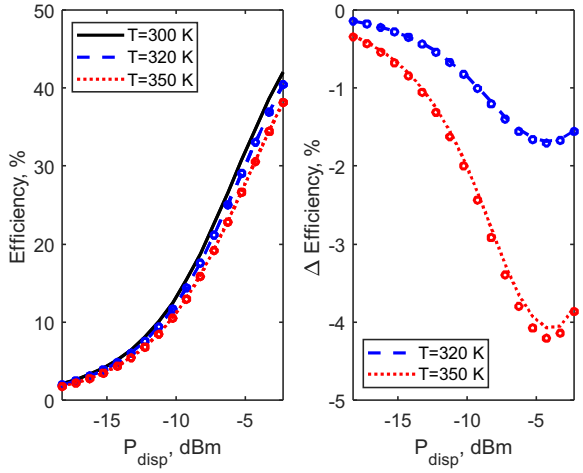

Fig. 6. Drain efficiency (left) and its variation with respect to the nominal temperature (right) as a function of the input power. Lines: incremental simulations at $T = 300$ K (solid), $T = 320$ K (dashed) and $T = 350$ K (dotted). Symbols: GF approach.

B. *T-dependent, Load-dependent Analysis*

We now extend the previous analysis to assess the overall power stage robustness against the concurrent variations of temperature and load termination (e.g. due to the variability of the matching network). Varying the real part of the optimum load by ± 5 % with respect to the nominal case (a range in line with EM simulations, see e.g. [5]), doubles the simulation time for the INC approach, while the GF analysis following (3) requires a negligible time overhead. Fig. 5 shows the dynamic load lines of the PA unit cell at 2 dB gain compression. The device is driven more harshly into compression by the increasing load (blue dashed lines), whereas the compression is lower in the opposite case, but the output swing is in any case reduced by the T-induced knee voltage increase. The accuracy of the time domain waveforms (DLL) shows that the harmonics are also well reproduced by the proposed GF T-dependent LS analysis. The $P_{\text{in}} - P_{\text{out}}$ and PAE reported in Fig. 7 also show examples of the concurrent load (here $+5\%$) and T variations.

Turning to the relative importance of the two variations, Fig. 8 reports the P_{out} and PAE variation with respect to their *nominal value* (i.e., $T = 300$ K and nominal load). In this figure, lines represent the variations due to temperature only, while the error bars represent the spread expected because of the $\pm 5\%$ load variations. Noticeably, the detailed variations depend on the input power: with larger load ($+5\%$), for example, P_{out} in back-off exhibits a lower reduction with respect to the nominal load (higher power and higher gain), while the opposite is true at higher input power since the compression is greater (see again Fig. 5). Furthermore the load sensitivity is lower in compression, again due to the reduced effect of the load termination at the knee. PAE has the highest load sensitivity close to the onset of gain compression (here around -7 dBm), but variations with temperature are in any case dominating, leading to a significant PAE reduction in a wide range of output power (as already noticed, roughly

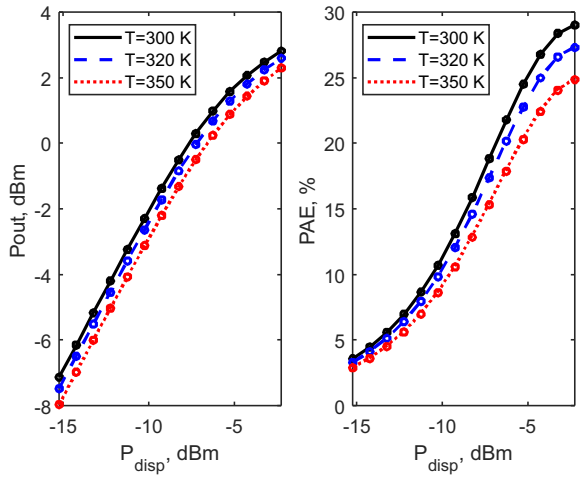

Fig. 7. Output power (left) and PAE (right) with varied load (+5% real part) and at different temperatures. Solid lines: incremental simulations. Symbols: GF approach with concurrent T and load variations according to (3).

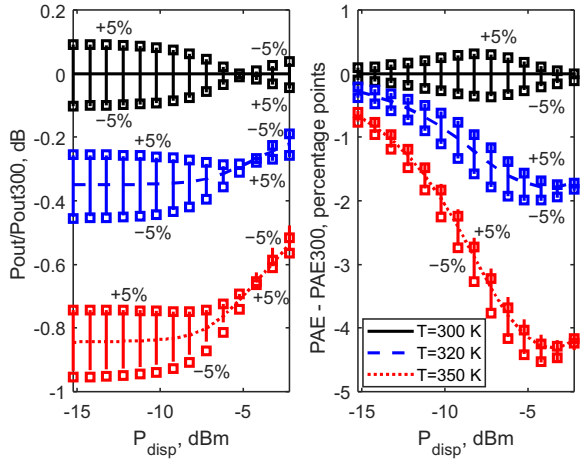

Fig. 8. Variation of the output power (left) and PAE (right) with temperature and load. Lines: incremental simulations with nominal load and $T = 300$ K (solid), $T = 320$ K (dashed) and $T = 350$ K (dotted). Error bars denote the expected spread due to ± 5 % variation of $\mathrm{Re}(Z_\mathrm{L})$ evaluated with the incremental analysis. Symbols: spread due to ± 5 % variation of $\mathrm{Re}(Z_\mathrm{L})$ following the GF approach with concurrent temperature and load variations.

from 5 dB OBO to saturation). All these intermixed effects are correctly reproduced by the GF analysis. Overall, the stage exhibits a spread of roughly 1 dB for P_out and 5 percentage points for PAE.

IV. Conclusion

A novel TCAD approach for the efficient temperature dependent analysis of nonlinear stages has been validated in a FinFET-based power amplifier along with the effect of concurrent load variations. The thermal degradation is shown to affect all the operating conditions, including the back-off case. The proposed approach demonstrates that LS TCAD analysis is mature for the assessment of nonlinear circuits and represents a first step towards the development of physically sound, temperature dependent, LS circuit models.

Acknowledgment

This work has been supported by the Italian MIUR PRIN 2017 Project "Empowering GaN-on-SiC and GaN-on-Si technologies for the next challenging millimeter-wave applications (GANAPP)"

References

[1] B. Troyanovsky, Z. Yu, and R. W. Dutton, "Large signal frequency domain device analysis via the harmonic balance technique," in *Simulation of Semiconductor Devices and Processes*. Springer Vienna, 1995, pp. 114–117.

[2] F. M. Rotella, G. Ma, Z. Yu, and R. W. Dutton, "Design optimization of RF power MOSFET's using large signal analysis device simulation of matching networks," in *Simulation of Semiconductor Processes and Devices 1998*. Springer Vienna, 1998, pp. 26–29.

[3] J. Fang, J. Moreno, R. Quaglia, V. Camarchia, M. Pirola, S. Donati Guerrieri, C. Ramella, and G. Ghione, "3.5 GHz WiMAX GaN doherty power amplifier with second harmonic tuning," *Microwave and Optical Technology Letters*, vol. 54, no. 11, pp. 2601–2605, 2012.

[4] S. Donati Guerrieri, F. Bonani, and G. Ghione, "Linking X parameters to physical simulations for design-oriented large-signal device variability modeling," in *2019 IEEE MTT-S International Microwave Symposium (IMS)*. IEEE, jun 2019.

[5] S. Donati Guerrieri, C. Ramella, F. Bonani, and G. Ghione, "Efficient sensitivity and variability analysis of nonlinear microwave stages through concurrent TCAD and EM modeling," *IEEE Journal on Multiscale and Multiphysics Computational Techniques*, vol. 4, pp. 356–363, 2019.

[6] S. Donati Guerrieri, F. Bonani, F. Bertazzi, and G. Ghione, "A unified approach to the sensitivity and variability physics-based modeling of semiconductor devices operated in dynamic conditions—Part I: Large-signal sensitivity," *IEEE Transactions on Electron Devices*, vol. 63, no. 3, pp. 1195–1201, mar 2016.

[7] ——, "A unified approach to the sensitivity and variability physics-based modeling of semiconductor devices operated in dynamic conditions.—Part II: Small-signal and conversion matrix sensitivity," *IEEE Transactions on Electron Devices*, vol. 63, no. 3, pp. 1202–1208, mar 2016.

[8] S. Donati Guerrieri, M. Pirola, and F. Bonani, "Concurrent efficient evaluation of small-change parameters and green's functions for TCAD device noise and variability analysis," *IEEE Transactions on Electron Devices*, vol. 64, no. 3, pp. 1269–1275, mar 2017.

[9] C. Prasad, "A review of self-heating effects in advanced CMOS technologies," *IEEE Transactions on Electron Devices*, vol. 66, no. 11, pp. 4546–4555, nov 2019.

[10] F. Bonani, V. Camarchia, F. Cappelluti, S. Donati Guerrieri, G. Ghione, and M. Pirola, "When self-consistency makes a difference," *IEEE Microwave Magazine*, vol. 9, no. 5, pp. 81–89, oct 2008.

[11] A. Benvenuti, W. M. Coughran, and M. R. Pinto, "A thermal-fully hydrodynamic model for semiconductor devices and applications to III-v HBT simulation," *IEEE Transactions on Electron Devices*, vol. 44, no. 9, pp. 1349–1359, 1997.

[12] E. Catoggio, S. Donati Guerrieri, and F. Bonani, "Efficient TCAD thermal analysis of semiconductor devices," *IEEE Transactions on Electron Devices*, 2021.

[13] S. Donati Guerrieri, F. Bonani, and G. Ghione, "A comprehensive technique for the assessment of microwave circuit design variability through physical simulations," in *2017 IEEE MTT-S International Microwave Symposium (IMS)*. IEEE, jun 2017.

[14] J.-P. Raskin, "FinFET versus UTBB SOI — a RF perspective," in *2015 45th European Solid State Device Research Conference (ESSDERC)*. IEEE, sep 2015.

[15] A. M. Bughio, S. Donati Guerrieri, F. Bonani, and G. Ghione, "Multi-gate FinFET mixer variability assessment through physics-based simulation," *IEEE Electron Device Letters*, vol. 38, no. 8, pp. 1004–1007, aug 2017.